

# Induced Kramer-Pesch-Effect in a Two Gap Superconductor: Application to MgB<sub>2</sub>

A. Gumann, S. Graser, T. Dahm, and N. Schopohl  
*Institut für Theoretische Physik, Universität Tübingen*  
*Auf der Morgenstelle 14, D-72076 Tübingen, Germany*  
(Dated: 21st November 2005)

The size of the vortex core in a clean superconductor is strongly temperature dependent and shrinks with decreasing temperature, decreasing to zero for  $T \rightarrow 0$ . We study this so-called Kramer-Pesch effect both for a single gap superconductor and for the case of a two gap superconductor using parameters appropriate for Magnesium Diboride. Usually, the Kramer-Pesch effect is absent in the dirty limit. Here, we show that the Kramer-Pesch effect exists in both bands of a two gap superconductor even if only one of the two bands is in the clean limit and the other band in the dirty limit, a case appropriate for MgB<sub>2</sub>. In this case an induced Kramer-Pesch effect appears in the dirty band. Besides numerical results we also present an analytical model for the spatial variation of the pairing potential in the vicinity of the vortex center that allows a simple calculation of the vortex core radius even in the limit  $T \rightarrow 0$ .

PACS numbers: 74.20.-z, 74.25.Bt, 74.70.Ad

## I. INTRODUCTION

In 1974 Kramer and Pesch theoretically discovered an unusual core shrinkage of an isolated vortex for decreasing temperature which they did not only observe in numerical solutions of Eilenberger's equations but also proved analytically [1]. While all other lengthscales describing the superconducting state, especially the London penetration depth and the coherence length, reach a saturation value with decreasing temperature, this investigation introduced a new lengthscales in the discussion of the vortex state of clean superconductors. It can be defined as the inverse of the slope of the pairing potential at the vortex center and describes not only the spatial variation of the gap function but also the maximum height of the supercurrent density around the vortex center and thus measures the size of the vortex core. In a clean superconductor without impurity scattering this length  $\xi_v$  decreases linearly with temperature tending to zero for  $T \rightarrow 0$  while in superconductors with larger scattering rates it reaches a saturation value. A detailed study of the impurity effect on the vortex core shrinkage can be found in Ref. [2].

It appears well established both experimentally and theoretically that the new superconductor MgB<sub>2</sub> is a two gap superconductor, possessing two superconducting gaps of significantly different size on disconnected parts of the Fermi surface [3, 4, 5, 6]. There exist other compounds, in which two gap superconductivity is believed to be realized, however, at present MgB<sub>2</sub> is the clearest example. In the case of such a multi band superconductor with several distinct gap values there exist different lengthscales that describe the spatial variation of the quasiparticle excitations corresponding to the different gap values. Therefore, we also expect different lengthscales for the description of the increase of the gap functions near the center of an isolated vortex in each band. It is obvious that these lengthscales are not inde-

pendent of each other if there is a coupling of the different bands via the pairing interaction. In this work we want to examine numerically the vortex core shrinkage for a two gap superconductor at the example of Magnesium Diboride. We also present an analytical gap model that well describes the low temperature behaviour of the core size  $\xi_v$ . In the last section we want to discuss a model of a two gap superconductor assuming large and small scattering rates in the different bands and its influence on the size of the vortex core.

## II. THE SINGLE BAND CASE

In this section, we study the vortex core structure of a standard (single band) superconductor. In the first subsection (II A), we describe how the Riccati parametrization formalism of the Eilenberger theory can be used to numerically calculate the structure of an isolated Abrikosov vortex in the clean limit. In the second subsection (II B), we present an analytical model for the pairing potential in the vicinity of an isolated Abrikosov vortex and explain how it can be used to calculate the temperature dependence of the vortex core size. The third subsection (II C) applies to the dirty limit. We point out how the theoretical description simplifies in this special case and discuss the results for the vortex core size.

### A. Numerical Calculations

In order to calculate the pairing potential  $\Delta(\vec{r}, T)$  for a certain region in real space, one has to find a solution to the gap equation:

$$\Delta(\vec{r}, T) = VN(0)2\pi T \sum_{0 < \varepsilon_n < \omega_c} \langle f(\vec{r}, \vec{k}_F, i\varepsilon_n) \rangle_{FS} \quad (1)$$

According to Refs. [7, 8], the quasiclassical propagator  $f(\vec{r}, \vec{k}_F, i\varepsilon_n)$  can be expressed in terms of two complex quantities  $a(x)$  and  $b(x)$ , called the Riccati amplitudes:

$$f(\vec{r}(x), \vec{k}_F, i\varepsilon_n) = \frac{2a(x)}{1 + a(x)b(x)} \quad (2)$$

The Riccati amplitudes  $a(x)$  and  $b(x)$  are in turn solutions to the Riccati differential equations

$$\hbar v_F \partial_x a(x) + [2\tilde{\varepsilon}_n + \Delta^\dagger(\vec{r}(x)) a(x)] a(x) - \Delta(\vec{r}(x)) = 0 \quad (3a)$$

$$\hbar v_F \partial_x b(x) - [2\tilde{\varepsilon}_n + \Delta(\vec{r}(x)) b(x)] b(x) + \Delta^\dagger(\vec{r}(x)) = 0 \quad (3b)$$

The Riccati differential equations have to be solved along real space trajectories  $\vec{r}(x)$  pointing in the direction of the Fermi wave vector  $\vec{v}_F(\vec{k}_F)$  using the modified Matsubara frequencies  $i\tilde{\varepsilon}_n = i\varepsilon_n + (e/c) \vec{v}_F \cdot \vec{A}(\vec{r}(x))$ . The quasiclassical Green's function  $f(\vec{r}, \vec{k}_F, i\varepsilon_n)$  calculated with the Riccati amplitudes according to equation (2) then has to be averaged over the Fermi surface of the superconducting material (denoted with  $\langle \dots \rangle_{FS}$ ).

As initial values for the integration of the Riccati differential equations the bulk values of the Riccati amplitudes have to be used ( $\varepsilon_n > 0$ ):

$$a(-\infty) = \frac{\Delta(-\infty)}{\varepsilon_n + \sqrt{\varepsilon_n^2 + |\Delta(-\infty)|^2}} \quad (4a)$$

$$b(+\infty) = \frac{\Delta^\dagger(+\infty)}{\varepsilon_n + \sqrt{\varepsilon_n^2 + |\Delta(+\infty)|^2}} \quad (4b)$$

The quasiclassical Green's function  $f(\vec{r}, \vec{k}_F, i\varepsilon_n)$  is, via the Riccati amplitudes, a function of the pairing potential. A straightforward way to find a solution to the self-consistency problem posed by the gap equation is to choose a certain initial configuration for the pairing potential  $\Delta(\vec{r}, T)$  and then improve this configuration iteratively.

Since we will apply the methods described in this chapter to study the temperature dependence of the vortex core size of an isolated Abrikosov vortex, it is convenient to define, at this point, a characteristic lengthscale for the size of the vortex core. We take up the proposal for a definition by Hayashi et al. [2]:

$$\xi_v^{-1} = \left. \frac{\partial \Delta(r)}{\partial r} \right|_{r=0} \frac{1}{\Delta(r=\infty, T)} \quad (5)$$

This characteristic lengthscale  $\xi_v$  corresponds to the inverse slope of the pairing potential  $\Delta(\vec{r}, T)$  at the vortex center  $r = 0$ , normalized to the bulk value of the pairing potential  $\Delta(r = \infty, T)$  at the corresponding temperature  $T$  and has to be distinguished from the bulk coherence length  $\xi_\infty = \hbar v_F / \Delta(r = \infty, T)$ .

Once a self-consistent solution for the pairing potential is found, the local quasiparticle spectrum  $N(\vec{r}, E)$  (local

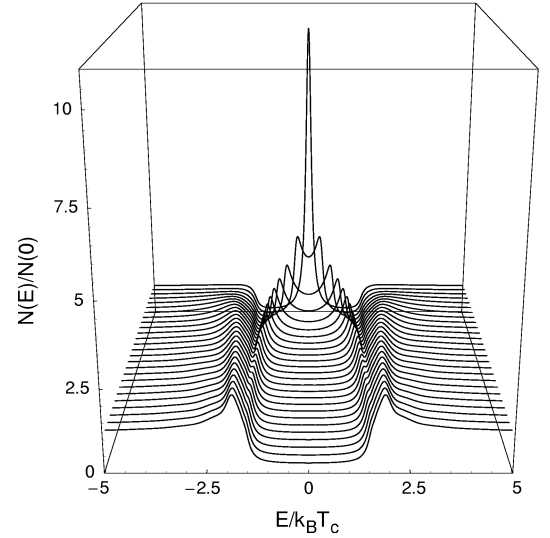


Figure 1: The quasiparticle spectrum in the single band case, plotted for several distances from the vortex core at a temperature of  $T = 0.5 T_c$ . The distances span from  $r = 0$  (rearmost curve) to  $r = 5 \xi_\infty$  (foremost curve) in steps of  $0.2 \xi_\infty$ . For these plots, an imaginary part (broadening) of  $\delta = 0.1$  was used.

density of states) can be calculated in the following manner:

$$N(\vec{r}, E) = \left\langle \text{Re} \left[ \frac{1 - ab}{1 + ab} \right]_{i\varepsilon_n \rightarrow E + i\delta} \right\rangle_{FS} \quad (6)$$

In Fig. 1, we show numerical results for the quasiparticle spectrum in the single band case. The curves were obtained evaluating Eq. (6) based on self-consistently calculated data for the pairing potential  $\Delta(\vec{r}, T)$  and a cylindrical Fermi surface has been assumed. A distinct zero energy peak represents Andreev bound states in the vortex core. For increasing distance from the vortex core, this peak splits and finally merges into the gap edges. Similar results have been obtained before. Gygi and Schlüter solved the Bogoliubov-de Gennes equations as an eigenvalue problem to study the electronic structure of a vortex line, see Ref. [9]. Ichioka et al. used the quasiclassical Eilenberger theory to examine the same problem, see Ref. [10].

Although the Riccati parametrization of the Eilenberger propagator offers a convenient and stable method to solve the Eilenberger equations and to calculate the local density of states, the effort of numerical calculations increases under certain circumstances. Firstly, as the lengthscale on which the pairing potential  $\Delta(\vec{r}, T)$  varies is getting shorter, the number of grid points on which the gap equation has to be solved in real space grows. Secondly, the number of terms in the sum over Matsubara frequencies  $\sum_{0 < \varepsilon_n < \omega_c}$  grows linearly with decreasing temperature. Thirdly, the averaging over all Fermi wave vectors  $\vec{v}_F$  that appear on the Fermi surface becomes la-

borious for complicated Fermi surface topologies.

Taking all these points into account, it is obvious that an analytical approach should be considered whenever possible, in particular if one wants to study the  $T \rightarrow 0$  limit. In the next chapter, this will be done for an isolated Abrikosov vortex.

### B. Exact Solution for an Analytical Gap Model

In the innermost part of an Abrikosov vortex, the modulus of the pairing potential grows linearly with increasing distance from the vortex center. As it approaches the bulk value, it saturates with a certain profile. Superimposed to the behaviour of the modulus of the pairing potential, the phase varies by  $2\pi$  around the vortex. This leads to the general form  $\Delta(\vec{r}) \sim r e^{i\phi}$  for the innermost part of the vortex, while in the outermost part, the behaviour  $\Delta(\vec{r}) \sim e^{i\phi}$  holds ( $r$  and  $\phi$  are polar coordinates in real space). Thus, the following simple analytical model for the pairing potential in the vicinity of an isolated Abrikosov vortex is useful:

$$\Delta(\vec{r}, T) = \begin{cases} \frac{\Delta_\infty(T)}{\xi_v} r e^{i\phi} & , r < \xi_v \\ \Delta_\infty(T) e^{i\phi} & , r \geq \xi_v \end{cases} \quad (7)$$

Here,  $\Delta_\infty(T)$  denotes the value of the pairing potential in the bulk at a given temperature  $T$ ;  $\xi_v$  is the length-scale on which the pairing potential rises from zero in the center of the vortex to the bulk value  $\Delta_\infty(T)$  and coincides with the previous definition (5). According to Ref. [8], every real space trajectory  $\vec{r}(x)$  is parametrized by an impact parameter  $y$  and the position along the trajectory  $x$ . In our special case, the impact parameter  $y$  is given by the distance from the trajectory to the vortex core. The position along the trajectory  $x$  is measured relative to the point closest to the vortex core. It follows from what has been said that

$$r e^{i\phi} = (x + iy) e^{i\theta} \quad (8)$$

along a chosen trajectory specified by  $\theta$ , the angle corresponding to the direction of the Fermi velocity in the  $ab$ -plane. Within the scope of this model, the pairing potential consists of a vortex core with a linear profile and a phase vortex in the circumference.

In the next two subsections, we will show how an analytical solution can be obtained for the quasiclassical Green's function in the special case of this particular pairing potential profile. We will then use this analytical solution in order to determine the lengthscale  $\xi_v$  self-consistently with the gap equation.

#### 1. Analytical Solution for $r < \xi_v$

In general, the linearized Bogoliubov-de Gennes equations, often referred to as Andreev equations, read

$$-i\hbar v_F \frac{\partial}{\partial x} \begin{bmatrix} u(x) \\ v(x) \end{bmatrix} = \begin{bmatrix} i\tilde{\varepsilon}_n(x) & -\Delta(x) \\ \Delta^\dagger(x) & -i\tilde{\varepsilon}_n(x) \end{bmatrix} \begin{bmatrix} u(x) \\ v(x) \end{bmatrix} \quad (9)$$

According to Ref. [8], the solutions of (9) are connected to the Riccati amplitude  $a(x)$  via

$$a(x) = i \frac{u(x)}{v(x)} \quad (10)$$

whereas the Riccati amplitude  $b(x)$  can be obtained applying the symmetry relation

$$b(x) = -a(-x) e^{-2i\theta} \quad (11)$$

which is valid if only a single vortex line is present. It should be noted that we do not solve the linearized Bogoliubov-de Gennes equations (9) as an eigenvalue problem, but as an initial value problem, see Ref. [8]. For the linear profile, Eq. (9) reads

$$\left\{ i\hbar v_F \partial_x + e^{i\frac{\theta}{2}\hat{\tau}_3} \left[ i\varepsilon_n \hat{\tau}_3 - \frac{\Delta_\infty}{\xi_v} i(x\hat{\tau}_2 + y\hat{\tau}_1) \right] e^{-i\frac{\theta}{2}\hat{\tau}_3} \right\} \circ \begin{pmatrix} u(x) \\ v(x) \end{pmatrix} = \hat{0} \quad (12)$$

where  $\hat{\tau}_i$  are the Pauli matrices. Applying the gauge transformation

$$\hat{\Psi}(x) = \begin{pmatrix} \Psi_1(x) \\ \Psi_2(x) \end{pmatrix} = e^{-i\frac{\theta}{2}\hat{\tau}_3} \circ \begin{pmatrix} u(x) \\ v(x) \end{pmatrix} \quad (13)$$

and introducing the spinor  $\hat{\Phi}(x)$  via

$$\hat{\Psi}(x) = \left( \hbar v_F \partial_x - \varepsilon_n \hat{\tau}_3 + \frac{\Delta_\infty}{\xi_v} (x\hat{\tau}_2 + y\hat{\tau}_1) \right) \circ e^{i\frac{\pi}{4}\hat{\tau}_1} \circ \hat{\Phi}(x) \quad (14)$$

one obtains the following two decoupled differential equations for the components  $\hat{\Phi}(x) = (\Phi_-(x), \Phi_+(x))^T$

$$\left[ (\hbar v_F \partial_x)^2 - \varepsilon_n^2 - \frac{\Delta_\infty^2}{\xi_v^2} (x^2 + y^2) \pm \hbar v_F \frac{\Delta_\infty}{\xi_v} \right] \circ \Phi_\mp(x) = 0 \quad (15)$$

Scaling the variables  $\bar{x} = \frac{x}{\xi}$  and  $\bar{y} = \frac{y}{\xi}$  to the characteristic lengthscale  $\xi = \sqrt{\frac{\xi_v \xi_\infty}{2}}$  with  $\xi_\infty = \frac{\hbar v_F}{\Delta_\infty}$  and introducing

$$\Phi_\pm(x) = \left( \frac{\xi}{\hbar v_F} \right)^2 \bar{\Phi}_\pm(\bar{x}) \quad (16)$$

$$c_\pm = \frac{1}{4} \left( \frac{\xi_v \varepsilon_n}{\xi \Delta_\infty} \right)^2 + \frac{1}{4} \bar{y}^2 \pm \frac{1}{2} \quad (17)$$

Eqs. (15) assume the following compact and dimensionless form:

$$\left[ \partial_{\bar{x}}^2 - c_{\pm} - \frac{1}{4} \bar{x}^2 \right] \bar{\Phi}_{\pm}(\bar{x}) = 0 \quad (18)$$

The general solution of this second order differential equation is given by a linear combination of the parabolic cylinder functions  $U(c_{\pm}, \bar{x})$  and  $V(c_{\pm}, \bar{x})$  [11]. We choose the following ansatz

$$\begin{aligned} \bar{\Phi}_{-}(\bar{x}) &= A_{-} V(c_{-}, -\bar{x}) \Theta(-\bar{x}) + B_{-} V(c_{-}, \bar{x}) \Theta(\bar{x}) \\ \bar{\Phi}_{+}(\bar{x}) &= A_{+} U(c_{+}, -\bar{x}) \Theta(-\bar{x}) + B_{+} U(c_{+}, \bar{x}) \Theta(\bar{x}) \end{aligned} \quad (19)$$

$$\text{with } \Theta(\bar{x}) = \begin{cases} 1 & \text{for } \bar{x} > 0 \\ 0 & \text{for } \bar{x} < 0 \end{cases}$$

in order to construct the Riccati amplitudes  $a(x)$  and  $b(x)$ . The connection between the Riccati amplitude  $a(x)$  and the solutions of the Andreev equation (12), given by (10), now reads

$$a(x) = \frac{\Psi_1(x)}{\Psi_2(x)} i e^{i\theta} \quad (20)$$

Let us briefly comment on the construction of the Riccati amplitudes  $a(x)$  and  $b(x)$ , respectively. A correct solution firstly has to solve the Riccati equations (3) and secondly has to possess the correct bulk asymptotics (4). The former is provided by construction [8] and we will see later on that the asymptotic behaviour obtained with this ansatz is indeed correct.

Additionally, it should be noted that the ansatz (19) is in fact unique. An expansion of the solution derived from the most general ansatz (containing both parabolic cylinder functions  $U(c_{\pm}, \bar{x})$  and  $V(c_{\pm}, \bar{x})$  for both functions  $\bar{\Phi}_{\pm}$  and all  $x$ ) exhibits the correct asymptotic behaviour if and only if the terms not contained in (19) vanish. Thus, the above form is being reproduced.

Using the ansatz (19), undoing the gauge transformation (13) and the substitutions (14), (16), then applying some basic properties of the parabolic cylinder functions [11] and making use of (20), one obtains the following expression for the Riccati amplitude  $a(\bar{x})$  for  $\bar{x} < 0$ :

$$a(\bar{x}) = e^{-i\theta} \frac{\left[ -\frac{V(c_{+}, -\bar{x})}{U(c_{-}, -\bar{x})} - \frac{1}{2} \left( \frac{\xi_v}{\xi} \frac{\varepsilon_n}{\Delta_{\infty}} - i\bar{y} \right) \frac{V(c_{-}, -\bar{x})}{U(c_{-}, -\bar{x})} \right] - \left( \frac{A_{+}}{iA_{-}} \right) \left[ 1 - \frac{1}{2} \left( \frac{\xi_v}{\xi} \frac{\varepsilon_n}{\Delta_{\infty}} + i\bar{y} \right) \frac{U(c_{+}, -\bar{x})}{U(c_{-}, -\bar{x})} \right]}{\left[ -\frac{V(c_{+}, -\bar{x})}{U(c_{-}, -\bar{x})} + \frac{1}{2} \left( \frac{\xi_v}{\xi} \frac{\varepsilon_n}{\Delta_{\infty}} - i\bar{y} \right) \frac{V(c_{-}, -\bar{x})}{U(c_{-}, -\bar{x})} \right] + \left( \frac{A_{+}}{iA_{-}} \right) \left[ 1 + \frac{1}{2} \left( \frac{\xi_v}{\xi} \frac{\varepsilon_n}{\Delta_{\infty}} + i\bar{y} \right) \frac{U(c_{+}, -\bar{x})}{U(c_{-}, -\bar{x})} \right]} \quad (21)$$

A similar expression can be obtained for  $\bar{x} > 0$ , but this will not be necessary for our further calculations. The Riccati amplitude  $b(\bar{x})$  for  $\bar{x} > 0$  can be constructed from equation (21) using the symmetry relation (11). We now have to determine the coefficient  $(\frac{A_{+}}{iA_{-}})$  in order to complete the solution. This will be achieved by matching Eq. (21) to the solution for  $r \geq \xi_v$ .

## 2. Analytical Solution for $r \geq \xi_v$

The outer region of our model for the pairing potential (7) is nothing but a pure phase vortex. Unfortunately, there is no exact solution to the Riccati equations (3) for such a phase vortex for all energies and all impact parameters. On the one hand, an exact solution for all values of the impact parameter can be obtained for the special case  $i\varepsilon_n \rightarrow E = |\Delta_{\infty}|$  [8]. On the other hand, an asymptotic solution for all energies is obvious for vanishing impact parameter (In this special case, the pairing potential is constant along any single trajectory except for the phase step in the vortex core). Since we will solve the gap equation for a real space position  $x_0$  that is very close to the vortex center (in fact we will perform the

limit  $x_0 \rightarrow 0$ ), the impact parameter will be vanishingly small in our calculations. Thus, we choose the asymptotic solution that is exact for all energies and vanishing impact parameter. It is of the following form:

$$a(\bar{x}) = \frac{|\Delta_{\infty}|}{\varepsilon_n + \sqrt{\varepsilon_n^2 + |\Delta_{\infty}|^2}} e^{i\phi} \quad (22)$$

Now the solution for the outer part of the vortex being constructed, we can demand that the solution be continuous at  $\xi_v$ . This means that Eq. (21) evaluated at  $x = \xi_v$  has to be equal to Eq. (22) which determines the coefficient  $(\frac{A_{+}}{iA_{-}})$ . Hence, we found a solution for the Riccati amplitudes for all positions  $x$  and all energies which is exact for vanishing impact parameter  $y$ .

We still have to check if the asymptotic behaviour of our solution is consistent with the bulk asymptotics of the Riccati amplitudes. These have been discussed in section (II A) and are given in Eqs. (4). On the one hand, we insert the linear profile of the pairing potential into Eqs. (4) and thus obtain the correct asymptotic behaviour. On the other hand, we move the matching point of our analytic solution to infinity and then expand Eq. (21) in terms of  $\bar{x} \rightarrow \pm\infty$ . Indeed, this reproduces the correct bulk asymptotics. With a finite matching point, par-

ticularly the matching point  $\xi_v$ , the correct asymptotic behaviour is provided by construction of the solution.

Altogether, we can therefore state that the solution constructed with ansatz (19) indeed exhibits the correct asymptotic behaviour in the bulk.

### 3. Solving the Gap Equation

In order to determine the lengthscale  $\xi_v$  on which the pairing potential rises from zero to the bulk value, we have to solve the gap equation (1) self-consistently for a real space position  $x_0$  which is close to the vortex center. Therefore, we have to calculate the quasiclassical Green's function  $f(\vec{r}, \vec{k}_F, i\varepsilon_n)$  according to Eq. (2) using the solutions for the Riccati amplitudes  $a(x)$  and  $b(x)$  we found in subsections (IIB1) and (IIB2). Since we are only interested in the lengthscale  $\xi_v$  which corresponds to the inverse slope of the pairing potential in the vortex core (see Eq. (5)), we differentiate the gap equation (1) at the vortex center  $x_0 = 0$  with respect to the position  $x_0$ :

$$\frac{\Delta_\infty(T)}{\xi_v} = VN(0)2\pi T \sum_{0 < \varepsilon_n < \omega_c} \langle \partial_{x_0} f(x_0 = 0) \rangle_{FS} \quad (23)$$

We now see that we only need to calculate the derivative of the Green's function  $f(\vec{r}, \vec{k}_F, i\varepsilon_n)$  at the vortex center:

$$\partial_{x_0} f(x_0 = 0) = \frac{\partial}{\partial x_0} \frac{2a}{1+ab} \Big|_{x_0=0} \quad (24)$$

We therefore only need to know the quantities  $a(x_0 = 0)$  and  $\partial_{x_0} a(x_0 = 0)$  which correspond to a vanishing impact parameter  $y$ . The Riccati amplitude  $b(x)$  can then be calculated using the symmetry relation (11). The expression obtained this way then has to be averaged over the Fermi surface (denoted by  $\langle \dots \rangle_{FS}$ ) and inserted into the gap equation. The lengthscale  $\xi_v(T)$  is, for the full temperature range, determined by this equation. Note that  $\xi_v$  still has to be determined self-consistently, because the Riccati amplitude  $a(x)$  depends on  $\xi_v$  via Eq. (21).

Fig. 2 shows the results from these calculations compared to those from a fully numerical self-consistent solution of the gap equation described in section (IIA). In both cases, a cylindrical Fermi surface has been used. The model for the pairing potential (7) yields a qualitatively correct behaviour of  $\xi_v(T)$  over the full temperature range. The lengthscale  $\xi_v$  diverges for  $T \rightarrow T_c$  and vanishes for  $T \rightarrow 0$ . In Fig. 3 we show the numerically determined gap profile together with the approximate one using the model given in Eq. (7). At low temperatures the slope at the vortex center is reproduced very well by the approximate model, while at higher temperatures deviations occur. This is reflected in the behaviour of the lengthscale  $\xi_v$  in Fig. 2.

Based on the analytical expressions obtained in this chapter, it is possible to calculate  $\xi_v$  in the limit  $T \rightarrow 0$

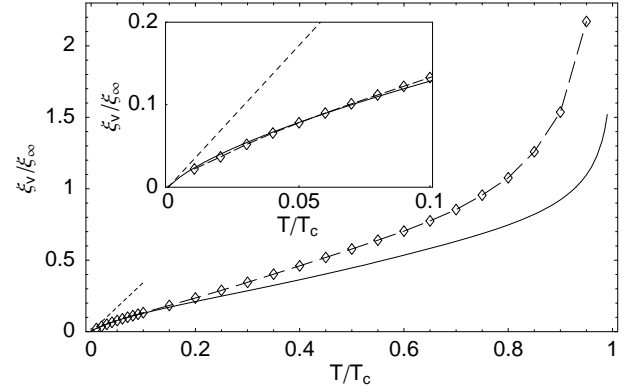


Figure 2: The lengthscale  $\xi_v(T)$  obtained from a linear profile of the pairing potential (solid line) and from a numerical self-consistent solution of the gap equation (diamonds with dashed guideline). Additionally, the plot shows the inclination of  $\xi_v$  in the limit  $T \rightarrow 0$  (dotted line). The inset is a blow-up of the low temperature region.

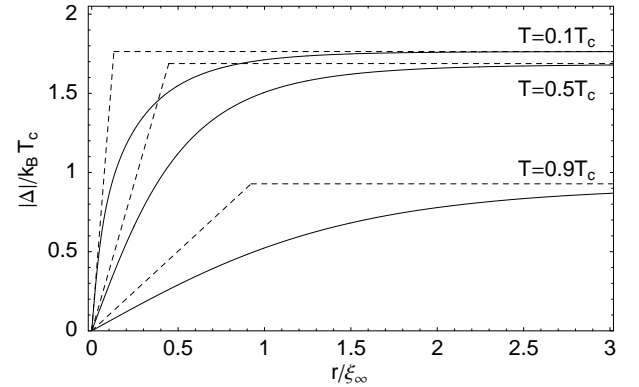


Figure 3: The modulus of the pairing potential as a function of the distance from the vortex center for three different temperatures. For each of the three different temperatures, we show the numerically determined self-consistent solution (solid line) and the linear profile with a slope calculated evaluating the gap equation at a position  $x_0 \rightarrow 0$  (dashed line). The matching of the slope at  $r = 0$  becomes very good at low temperatures.

as long as the cut-off frequency  $\omega_c$  is finite. Therefore, one has to insert the analytical result for the Riccati amplitude  $a(x)$  given in Eq. (21) into Eq. (24) making use of the symmetry relation (11); this quantity can then be inserted into the differentiated gap equation (23) and the limit  $T \rightarrow 0$  can be performed. The result is the following:

$$\xi_v \rightarrow \frac{4\xi_\infty}{\pi VN(0)\Delta_\infty} \frac{T}{T_c} \quad \text{for } T \rightarrow 0 \quad (25)$$

This leads to  $\xi_v \propto \xi_\infty T/T_c$  and we can thus, within the Riccati parametrization formalism of the Eilenberger theory, reproduce the result found earlier by Kramer and

Pesch [1] as a limiting case of our calculations.

It should be noted that the linear behaviour for  $T \rightarrow 0$  is valid only for a very narrow temperature range (see the inset in Fig. 2). The curve  $\xi_v(T)$  bends towards  $\xi_v = 0$  not until very low temperatures ( $\sim 0.05 T_c$ ). Thus, linear extrapolations from higher temperatures towards  $T = 0$  should be handled with care.

### C. Comparison with Dirty Limit Calculations

In the case of a dirty superconductor with high scattering rates the Eilenberger equations reduce to a simple diffusionlike equation for the Usadel propagator represented by the Green's functions  $G(\vec{r}, \varepsilon_n)$  and  $F(\vec{r}, \varepsilon_n)$  that are independent of the Fermi wave vector  $\vec{k}_F$  as was shown by Usadel [12]. Following the notation of Koshelev and Golubov in [13] this equation can be written as

$$\varepsilon_n F - \frac{\mathcal{D}}{2} \left[ G \left( \vec{\nabla} - \frac{2\pi i}{\Phi_0} \vec{A} \right)^2 F - F \vec{\nabla}^2 G \right] = \Delta G$$

together with the self-consistency condition

$$\Delta(\vec{r}) = VN(0) 2\pi T \sum_{0 < \varepsilon_n < \omega_c} F(\vec{r}, \varepsilon_n) \quad (26)$$

where we have assumed that the Fermi surface is rotationally symmetric with respect to the applied magnetic field and we have reduced the equations to the single band case. The characteristic lengthscale is determined by the diffusion constant  $\mathcal{D}$  and can be written as

$$\xi_\infty = \sqrt{\frac{\mathcal{D}}{2\pi T_c}} \quad (27)$$

Employing the normalization condition

$$[G(\vec{r}, \varepsilon_n)]^2 + F^\dagger(\vec{r}, \varepsilon_n) F(\vec{r}, \varepsilon_n) = 1$$

we can introduce a parametrization for the momentum averaged Usadel Green's functions  $G(\vec{r}, \varepsilon_n)$  and  $F(\vec{r}, \varepsilon_n)$  similar to the Riccati parametrization for the clean limit Eilenberger equations [14, 15].

$$G(\vec{r}, \varepsilon_n) = \frac{1 - a^2}{1 + a^2}, \quad F(\vec{r}, \varepsilon_n) e^{-i\varphi} = \frac{2a}{1 + a^2} \quad (28)$$

It should be noted that here we restricted to positive Matsubara frequencies  $\varepsilon_n > 0$ .

In the vicinity of an Abrikosov vortex we can simplify the equations by switching to cylindrical coordinates. If we assume a large Ginzburg-Landau parameter  $\kappa \gg 1$  and confine to an isolated vortex we can neglect the vector potential and write down the differential equation for  $a(r)$  as

$$2\varepsilon_n a - \mathcal{D} \left[ \frac{1}{r} \partial_r (r \partial_r a) - \frac{2a (\partial_r a)^2}{1 + a^2} - \frac{1}{r^2} \frac{a(1 - a^2)}{1 + a^2} \right] = (1 - a^2) \Delta(r) \quad (29)$$

Here  $r$  denotes the distance from the vortex center and the phase of the order parameter  $\varphi$  has been assumed to coincide with the polar angle  $\phi$  as  $\Delta(\vec{r}) = \Delta(r) e^{i\phi}$ . The parameter  $a(r)$  is related to the parameter  $\theta$  of [13] by  $a(r) = \tan \frac{\theta}{2}$ . Inserting this relation into Eq. (29) and normalizing all energies to  $\pi T_c$  and all lengths to  $\xi_\infty$  we reproduce the differential equation for  $\theta(r)$  from Ref. [13]:

$$\partial_r^2 \theta(r, \varepsilon_n) + \frac{1}{r} \partial_r \theta(r, \varepsilon_n) - \frac{1}{r^2} \cos \theta(r, \varepsilon_n) \sin \theta(r, \varepsilon_n) + \Delta(r) \cos \theta(r, \varepsilon_n) - \varepsilon_n \sin \theta(r, \varepsilon_n) = 0 \quad (30)$$

together with the gap equation

$$\Delta(r) = VN(0) 2\pi T \sum_{0 < \varepsilon_n < \omega_c} \sin \theta(r, \varepsilon_n) \quad (31)$$

The boundary conditions for the differential equation (30) follow from general considerations: In the vortex center the anomalous Green's function  $F(\vec{r}, \varepsilon_n)$  vanishes together with the modulus of the pairing potential leading to

$$\theta(r = 0, \varepsilon_n) = 0 \quad (32)$$

and far from the vortex center we expect the Green's functions to assume their bulk values and we obtain

$$\theta(r \rightarrow \infty, \varepsilon_n) = \arctan \frac{\Delta_0}{\varepsilon_n} \quad (33)$$

To obtain a self-consistent profile for the pairing potential  $\Delta(r)$  the Usadel equations have to be solved iteratively together with the gap equation as described in section (II A). We used a relaxation method for a fast and stable solution of the boundary value problem defined by Eqs. (30, 32, 33) and chose a cut-off for the Matsubara frequency summation in Eq. (31) of  $\omega_c = 20\pi T_c$ . Extracting the characteristic length  $\xi_v$  from the inverse slope of the pairing potential in the vortex center we find – as expected from several other calculations, e.g. [2] – a saturation value of  $\xi_v$  for low temperatures, see Fig. 4, i.e. in the dirty limit the Kramer-Pesch effect disappears.

In Fig. 5, we show the quasiparticle spectrum calculated as the real part of the analytical continuation of the Usadel Green's function  $G(\vec{r}, -iE + \delta)$  according to Eq. (30). Due to strong impurity scattering, the zero energy bound state in the vortex core is replaced by a flat normal state spectrum.

### III. THE TWO GAP CASE

In this section, we study the vortex core structure of a two gap superconductor. In the first subsection (III A), we explain how the numerical procedure for the single band case from section (II A) can be generalized in order to describe a clean two band system. In the second subsection (III B), we do the same for the analytical model for the pairing potential from section (II B). In this subsection, we also present results for a two gap superconductor in the dirty limit.

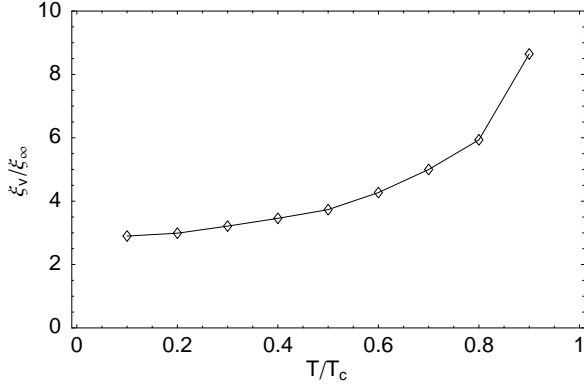


Figure 4: The lengthscale  $\xi_v(T)$  for the dirty limit approach. A saturation occurs at low temperatures.

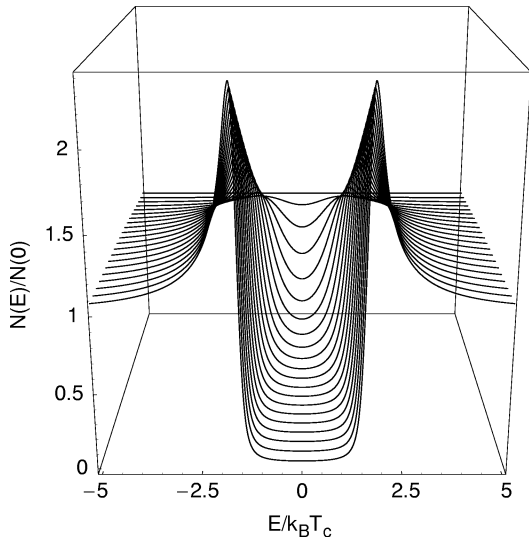


Figure 5: The quasiparticle spectrum in the dirty limit, plotted for several distances from the vortex core at a temperature of  $T = 0.5 T_c$ . The distances span from  $r = 0$  (rearmost curve) to  $r = 10 \xi_\infty$  (foremost curve) in steps of  $0.5 \xi_\infty$ .

### A. Numerical Calculations

In order to include two band behaviour into our considerations, the gap equation (1) has to be replaced by a two band gap equation:

$$\Delta^{(\alpha)}(\vec{r}, T) = 2\pi T \sum_{\alpha'} \lambda_{\alpha\alpha'} \sum_{0 < \varepsilon_n < \omega_c} \langle f_{\alpha'} \rangle_{FS, \alpha'} \quad (34)$$

with  $\alpha, \alpha' \in \{\sigma, \pi\}$

This two band gap equation can be derived starting from the fully momentum dependent multiband formulation of the quasiclassical (Eilenberger) theory [16] and has been used successfully to describe the upper critical field in MgB<sub>2</sub> [17]. We introduced two band indices ( $\sigma$  and  $\pi$ ) with respect to the usual nomenclature in MgB<sub>2</sub> as well

as a  $2 \times 2$  coupling matrix  $\lambda_{\alpha\alpha'}$ .

The application of the two band gap equation (34) requires the calculation of the quasiclassical Green's function for the two bands separately,  $f_\sigma(\vec{r}, \vec{k}_F, i\varepsilon_n)$  for the  $\sigma$  band and  $f_\pi(\vec{r}, \vec{k}_F, i\varepsilon_n)$  for the  $\pi$  band. Eqs. (2)-(4) still apply, but the  $\sigma$  component of the pairing potential  $\Delta^{(\sigma)}(\vec{r}, T)$  has to be used for the calculation of  $f_\sigma(\vec{r}, \vec{k}_F, i\varepsilon_n)$  and the  $\pi$  component  $\Delta^{(\pi)}(\vec{r}, T)$  for the calculation of  $f_\pi(\vec{r}, \vec{k}_F, i\varepsilon_n)$ , respectively.

Additionally, the Fermi surface topology of MgB<sub>2</sub> has to be taken into account in the Fermi surface averages  $\langle \dots \rangle_{FS, \sigma}$  and  $\langle \dots \rangle_{FS, \pi}$ , respectively. Band structure calculations have been carried out to determine the Fermi surface structure [3, 18] as well as microscopic calculations that revealed the distribution of the superconducting gap on the Fermi surface [4, 5]. Here, we use a simple model for the Fermi surface that has been suggested in Ref. [17]: a half-torus for the  $\pi$  band and a distorted cylinder for the  $\sigma$  band, respectively. This model correctly reproduces the Fermi surface topology and has proved to describe the upper critical field anisotropy in MgB<sub>2</sub>. This leads to the following integral parametrizations [17, 19]:

$$\begin{aligned} \langle \dots \rangle_{FS, \sigma} &= \frac{c}{4\pi^2} \int_{-\frac{\pi}{2}}^{\frac{\pi}{2}} dk_c \int_0^{2\pi} d\phi \dots \\ \langle \dots \rangle_{FS, \pi} &= \frac{1}{2\pi} \int_{\frac{\pi}{2}}^{\frac{3\pi}{2}} d\theta \int_0^{2\pi} d\phi \frac{1 + \kappa \cos \theta}{1 - 2\kappa/\pi} \dots \end{aligned} \quad (35)$$

Here,  $\phi \in [0, 2\pi]$  is the azimuthal angle within the  $ab$  plane,  $\theta \in [\frac{\pi}{2}, \frac{3\pi}{2}]$  the polar angle of the torus,  $k_c$  the  $c$ -axis component of the momentum,  $c$  the lattice constant in the  $c$ -axis direction, and  $\kappa = 0.25$  the ratio of the two radii of the torus [17].

In the two band gap equation (34), the coupling between the two bands occurs via the coupling matrix  $\lambda_{\alpha\alpha'}$  which, in the weak coupling limit, can be calculated from the ratio of the gap amplitudes for  $T \rightarrow 0$  ( $\Delta_\infty^{(\sigma)}/\Delta_\infty^{(\pi)}(T \rightarrow 0)$ ) and for  $T \rightarrow T_c$  ( $\Delta_\infty^{(\sigma)}/\Delta_\infty^{(\pi)}(T \rightarrow T_c)$ ), from the ratio of the densities of states in the normal (non-superconducting) state ( $N(0)^{(\sigma)}/N(0)^{(\pi)}$ ) and from the cut-off frequency  $\omega_c$  [20]. The ratio  $\Delta_\infty^{(\sigma)}/\Delta_\infty^{(\pi)}$  can be extracted from calculations of the two superconducting energy gaps based on the Eliashberg formalism as well as the ratio  $N(0)^{(\sigma)}/N(0)^{(\pi)}$  [5]. The values  $\Delta_\infty^{(\sigma)}/\Delta_\infty^{(\pi)}(T \rightarrow 0) = 3$ ,  $\Delta_\infty^{(\sigma)}/\Delta_\infty^{(\pi)}(T \rightarrow T_c) = 4$  and  $N(0)^{(\sigma)}/N(0)^{(\pi)} = 0.734$  have been used in our calculations.

The general form of the two band gap equation (34) leads to the complication that the two components of the pairing potential,  $\Delta^{(\sigma)}(\vec{r}, T)$  and  $\Delta^{(\pi)}(\vec{r}, T)$ , have to be calculated simultaneously.

In the case of a two band superconductor, the spectral distribution of quasiparticles  $N(\vec{r}, E)$  is the weighted sum of the spectral distribution for the  $\sigma$  band and for the  $\pi$

band, each of the two calculated according to Eq. (6):

$$N_{tot}(\vec{r}, T) = w_\sigma N_\sigma(\vec{r}, E) + w_\pi N_\pi(\vec{r}, E) \quad (36)$$

For the special case of  $\text{MgB}_2$ , the weight of the spectral distribution of the  $\pi$  band  $w_\pi$  is given by  $w_\pi = N(0)^{(\pi)} / (N(0)^{(\sigma)} + N(0)^{(\pi)}) = 0.577$ , which implies  $w_\sigma = 1 - w_\pi = 0.423$  (e.g. see [3, 4]).

In Fig. 6, we show numerical results for the two band quasiparticle spectrum in the special case of  $\text{MgB}_2$ . The total quasiparticle spectrum exhibits much more structure due to the superposition of the spectra of the two single bands.

### B. The analytical Gap Model for Two Bands

In order to extend the analytical gap model from chapter (II B) to the case of a two gap superconductor, one has to introduce two separate gap models for the pairing potential, one for each band, and each of the two in the form of Eq. (7). Hence, one has to introduce two lengthscales, one for each of the two bands:  $\xi_v^{(\sigma)}$  and  $\xi_v^{(\pi)}$ . Following the discussion in section (III A), the calculations carried out in chapter (II B) have then to be repeated for each of the two bands separately in order to obtain the quasiclassical Green's function for both bands:  $f_\sigma(\vec{r}, \vec{k}_F, i\varepsilon_n)$  and  $f_\pi(\vec{r}, \vec{k}_F, i\varepsilon_n)$ . A coupling of the two bands first occurs in the gap equation (34).

In full analogy to the procedure in chapter (II B), the Green's function  $f(\vec{r}, \vec{k}_F, i\varepsilon_n)$  can be calculated for each of the two bands. The two band gap equation (34) can again be differentiated at the center of the vortex  $x_0 = 0$  with respect to the position  $x_0$  and determines the two lengthscales  $\xi_v^{(\sigma)}$  and  $\xi_v^{(\pi)}$  for the full temperature range:

$$\frac{\Delta_\infty^{(\alpha)}}{\xi_v^{(\alpha)}} = 2\pi T \sum_{\alpha'} \lambda_{\alpha\alpha'} \sum_{0 < \varepsilon_n < \omega_c} \langle \partial_{x_0} f_{\alpha'}(x_0 = 0) \rangle_{FS, \alpha'} \quad (37)$$

In Fig. 7, we show the results from these calculations, again compared to the results from a fully self-consistent solution of the two band gap equation. As in the single gap case, the linear profile for the pairing potential results in a qualitatively correct behaviour of  $\xi_v^{(\sigma)}(T)$  and  $\xi_v^{(\pi)}(T)$  for the full temperature range. The lengthscales  $\xi_v^{(\sigma)}$  and  $\xi_v^{(\pi)}$  diverge for  $T \rightarrow T_c$  and vanish for  $T \rightarrow 0$ . Thus, we find a Kramer-Pesch effect in both bands of a clean two band system. Again, for low temperatures the linear profile matches nicely the self-consistently calculated curve but shows deviations for higher temperatures. As in the single band case, the lengthscales  $\xi_v^{(\sigma)}$  and  $\xi_v^{(\pi)}$  bend towards  $\xi_v^{(\sigma)} = \xi_v^{(\pi)} = 0$  not until very low temperatures ( $\sim 0.05 T_c$ ) and thus one should again be careful with extrapolations from higher temperatures towards  $T = 0$  (see inset in Fig. 7).

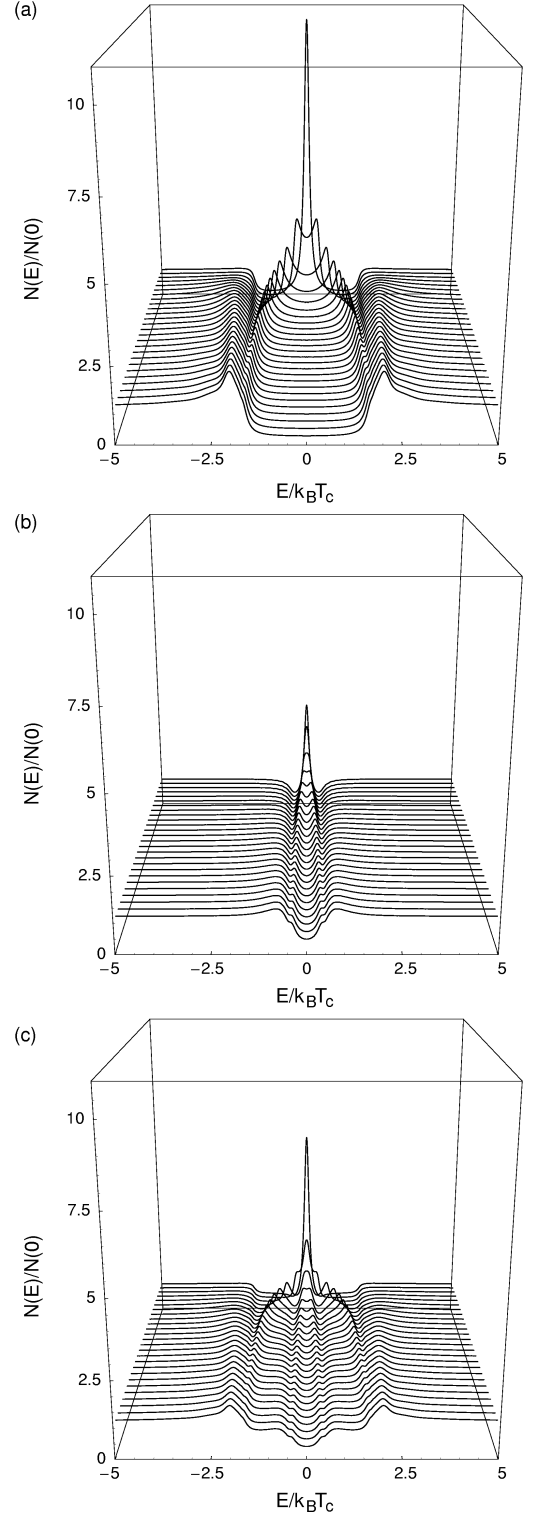


Figure 6: The quasiparticle spectrum in the two band case, again for several distances from the vortex core. (a) shows the quasiparticle spectrum of the  $\sigma$  band and (b) that of the  $\pi$  band. In (c), the total quasiparticle spectrum is being plotted. As before, the distances span from  $r = 0$  (rearmost curve) to  $r = 5 \xi_\infty$  (foremost curve) in steps of  $0.2 \xi_\infty$  and an imaginary part of  $\delta = 0.1$  was used.



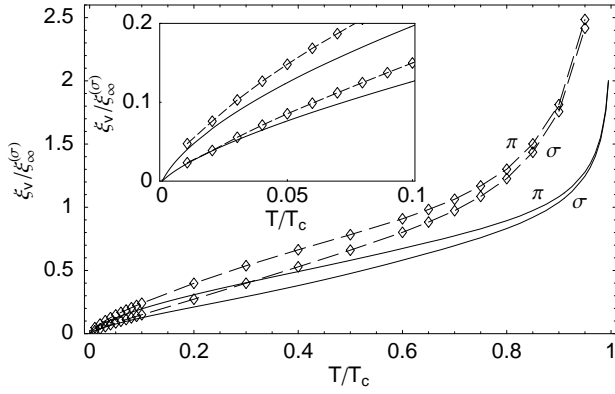


Figure 7: The lengthscales  $\xi_v^{(\sigma)}(T)$  and  $\xi_v^{(\pi)}(T)$  obtained from a linear profile of the pairing potential (solid line) and from a numerical self-consistent solution of the gap equation (diamonds with dashed guidelines). Inset: Blow-up of the low temperature region.

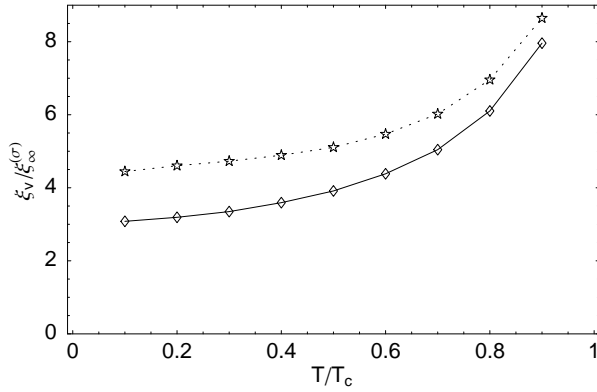


Figure 8: The numerical results for the vortex core radii  $\xi_v$  as a function of temperature for the  $\sigma$  band (diamonds) and the  $\pi$  band (stars) calculated in the dirty limit with a ratio of the diffusion constants  $\mathcal{D}^{(\sigma)} = 0.2\mathcal{D}^{(\pi)}$ . One can clearly see a saturation for low temperatures. The lines are guides for the eye.

We also show the comparison with a dirty limit calculation of the two band gap equation using the Usadel formalism introduced in section (II C), see Fig. 8. In this case we used slightly different parameters to calculate the coupling matrix  $\lambda_{\alpha\alpha'}$  than in the clean limit calculations. For the ratio of the diffusion constants we have chosen the value proposed by Koshelev and Golubov in [13] as  $\mathcal{D}^{(\sigma)} = 0.2\mathcal{D}^{(\pi)}$  leading to a ratio of the coherence lengths to be  $\xi_\infty^{(\sigma)} = 0.477\xi_\infty^{(\pi)}$ . As expected, we find a finite core size for both bands even for low temperatures and thus, as in the single gap case, no Kramer-Pesch effect exists in the dirty limit.

In order to compare the behaviour of the two bands, it is useful to study the ratio  $\xi_v^{(\pi)}/\xi_v^{(\sigma)}$ . In Fig. 9, we show this ratio for the clean and the dirty limit. The clean limit results were obtained, on the one hand, from a numeri-

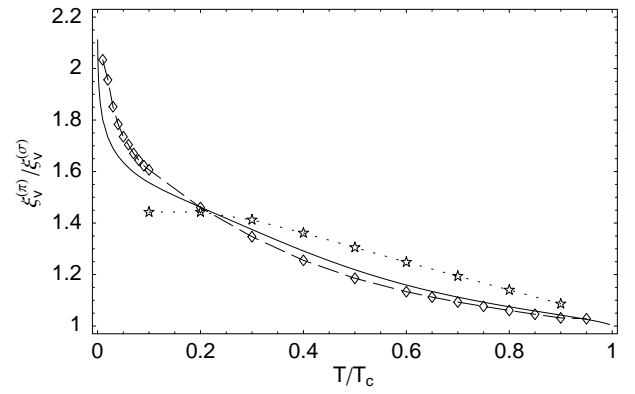


Figure 9: The ratio  $\xi_v^{(\pi)}/\xi_v^{(\sigma)}$  for the clean and the dirty limit. Solid line: results from the linear profile of the pairing potential for the clean limit. Diamonds with dashed guideline: numerical solution of the gap equation in the clean limit. Stars with dotted guideline: Usadel formalism results for the dirty limit.

cal solution of the gap equation and, on the other hand, from the analytical model for the pairing potential. The dirty limit results stem from calculations within the Usadel formalism. For high temperatures ( $T \rightarrow T_c$ ), both  $\xi_v^{(\pi)}$  and  $\xi_v^{(\sigma)}$  diverge and the ratio  $\xi_v^{(\pi)}/\xi_v^{(\sigma)}$  tends to 1 in the clean as well as in the dirty limit. For low temperatures ( $T \rightarrow 0$ ), the clean and the dirty limit results differ greatly. In the clean limit, both lengthscales vanish, however, in a way that leads to a strong growth of the ratio  $\xi_v^{(\pi)}/\xi_v^{(\sigma)}$ , i.e. the vortex core size in the  $\pi$  band decreases more slowly as a function of temperature than the one in the  $\sigma$  band. The agreement between the numerical results and those from the linear profile is very good here. In the dirty limit, the saturation of both  $\xi_v^{(\pi)}$  and  $\xi_v^{(\sigma)}$  leads to a saturation of the ratio  $\xi_v^{(\pi)}/\xi_v^{(\sigma)}$ .

The quasiparticle spectrum for two dirty bands is a simple superposition of two single band spectra as can be seen in Fig. 10.

#### IV. INDUCED KRAMER-PESCH EFFECT IN A DIRTY $\pi$ BAND

In present high-quality samples of  $\text{MgB}_2$  it is believed that the intraband scattering rate in the  $\sigma$  bands is smaller than the gap value, while in the  $\pi$  bands the intraband scattering rate is larger than the corresponding gap value [21, 22, 23]. Therefore we want to discuss in this section – as first suggested by M. Eschrig [24] – a model with a clean  $\sigma$  band and a dirty  $\pi$  band. Since the gap profiles in the two bands can not vary independently as they are coupled via the gap equation, we expect that for low temperatures they show the same asymptotic behaviour. But it is not at all clear if we find a decrease of  $\xi_v^{(\sigma)}$  and  $\xi_v^{(\pi)}$  for  $T \rightarrow 0$  as in the clean limit calculations or a saturation value as in the dirty limit approach. To

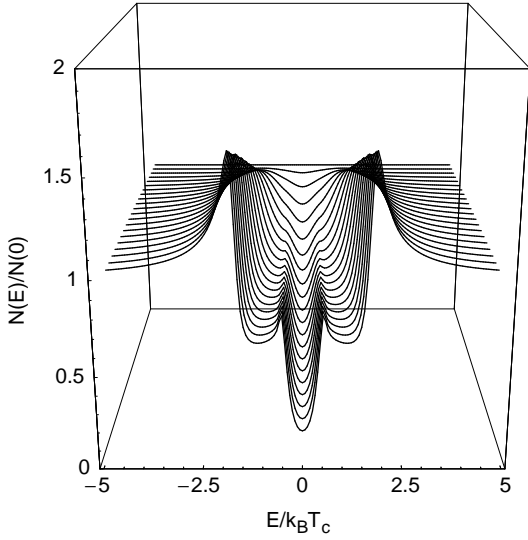


Figure 10: The quasiparticle spectrum in the two band dirty limit approach, again for several distances from the vortex core. As before, the distances span from  $r = 0$  (rearmost curve) to  $r = 10\xi_\infty$  (foremost curve) in steps of  $0.5\xi_\infty$ .

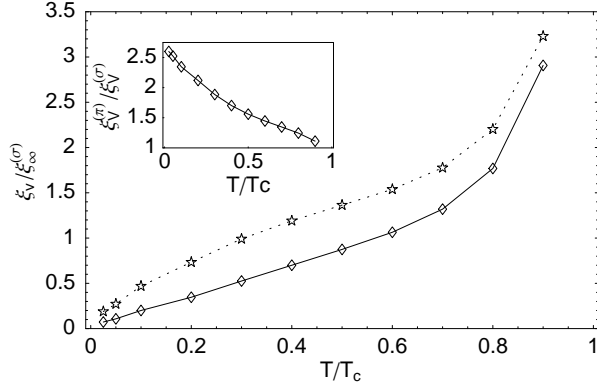


Figure 11: The numerical results for the vortex core radii  $\xi_v$  as a function of temperature for the clean  $\sigma$  band (diamonds) and the dirty  $\pi$  band (stars) calculated in a mixed model with equal coherence lengths in the two bands  $\xi_\infty^{(\sigma)} = \xi_\infty^{(\pi)}$ . The clean  $\sigma$  band and the dirty  $\pi$  band show both a significant Kramer-Pesch effect for low temperatures. The ratio of the core radii in the  $\pi$  and in the  $\sigma$  band as a function of temperature calculated for a clean  $\sigma$  and a dirty  $\pi$  band is shown in the inset. Again in both plots the lines are guides for the eye.

obtain a result for the two vortex core radii we have to solve the two band gap equation (34) where we calculate  $f_\sigma$  from the Riccati amplitudes  $a_\sigma$  and  $b_\sigma$  according to (2), while the Fermi surface averaged Green's function  $\langle f_\pi \rangle_{FS,\pi}$  is replaced by the Usadel Green's function  $F_\pi(\vec{r}, \varepsilon_n)$  that is a solution of a simple boundary value problem as described in section (II C). Since we have two different lengthscales in the clean and the dirty band case

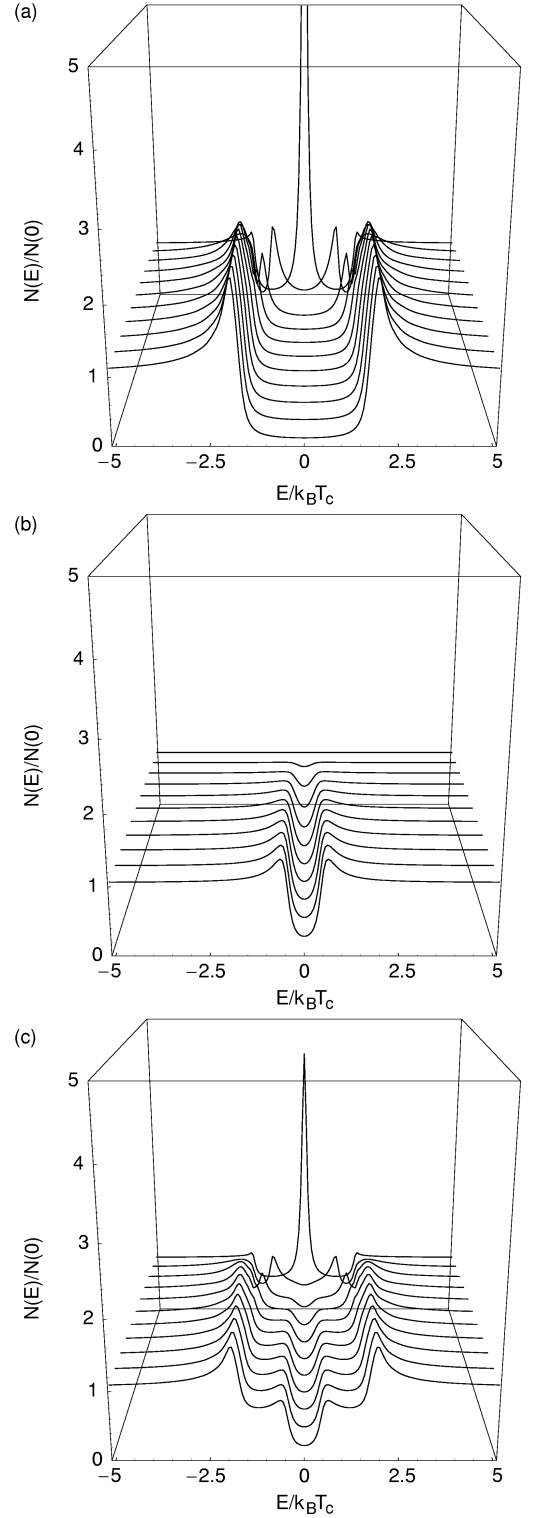


Figure 12: The quasiparticle spectrum in the two band case, again for several distances from the vortex core. Plot (a) shows the quasiparticle spectrum of the clean  $\sigma$  band and (b) that of the dirty  $\pi$  band. In (c), the total quasiparticle spectrum is being plotted for the mixed model. As before, the distances span from  $r = 0$  (rearmost curve) to  $r = 10\xi_\infty$  (foremost curve) in steps of  $\xi_\infty$  and an imaginary part of  $\delta = 0.1$  was used.

$\xi_{\infty}^{(\sigma)} = \frac{\hbar v_F}{\Delta_0^{(\sigma)}}$  and  $\xi_{\infty}^{(\pi)} = \sqrt{\frac{\mathcal{D}^{(\pi)}}{2\pi T_c}}$  we have to fix the ratio of the two coherence lengths which in general will depend on the sample quality, i.e. the scattering rate in the  $\pi$  band. Assuming the diffusion constant  $\mathcal{D}^{(\pi)}$  to be of the order of

$$\mathcal{D}^{(\pi)} \approx 2\pi T_c \left( \frac{\hbar v_F}{\Delta_0^{(\sigma)}} \right)^2$$

we chose the ratio to be  $\xi_{\infty}^{(\sigma)}/\xi_{\infty}^{(\pi)} = 1$ . We do not expect the essential qualitative results to depend on the special value of this ratio which we have checked numerically for a different ratio. In Fig. 11 we show the numerical results of this calculation. In our calculation we find a distinct decrease of the vortex core size for low temperatures even in the dirty  $\pi$  band, that can be understood as an induced Kramer-Pesch effect due to the real space coupling of the two gap amplitudes via the gap equation. The influence of the dirty  $\pi$  band is reflected in a larger ratio of  $\xi_v^{(\pi)}/\xi_v^{(\sigma)}$  for low temperatures than in the pure clean limit or the pure dirty limit approach.

In Fig. 12, we show the quasiparticle spectrum for the mixed model, consisting of a clean  $\sigma$  band and a dirty  $\pi$  band. Looking at the  $\sigma$  and  $\pi$  band spectra individually, it is obvious that the zero energy bound state only exists in the clean band. Thus, a zero energy peak is visible in the total quasiparticle spectrum, but it is lifted by an offset due to the flat spectrum of the dirty band. Restricting to the vortex core region, this leads to a picture that is very similar to the clean single band case.

## V. CONCLUSIONS

We have studied the Kramer-Pesch effect in both a single gap and a two gap superconductor using parameters relevant for  $\text{MgB}_2$ . We have presented a model for the

vortex core that allows an analytical solution for the Riccati equations in both cases and compared it with fully self-consistent numerical solutions. This model is useful for approximate calculations, in particular at low temperatures.

In the two gap case we find that the Kramer-Pesch effect is present in both bands in the clean limit. At high temperatures the sizes of the two components of the vortex core become equal, while at low temperatures the size of the vortex core in the  $\pi$  band with the smaller gap decreases more slowly with decreasing temperature.

We also investigated the dirty limit within the framework of the Usadel equations. In a single band superconductor there is no Kramer-Pesch effect in the dirty limit as has been discussed before [2]. However, in a two gap superconductor an interesting new situation arises, when one band is in the clean limit while the other is in the dirty limit, as is believed to be the case in high quality  $\text{MgB}_2$  samples. In this particular case we find that even in the dirty band a Kramer-Pesch effect exists, induced by the clean band.

Traditionally the Kramer-Pesch effect is difficult to observe experimentally due to the disturbing effect of impurities. Our calculations indicate that there is a better chance of observing this effect in  $\text{MgB}_2$  by scanning tunneling microscopy (STM) imaging of the vortex core as a function of temperature, because the  $\pi$  band may be in the dirty limit and still showing a decreasing vortex core size with decreasing temperature, as seen in Fig. 11.

## Acknowledgments

We would like to thank Christian Iniotakis, Nobuhiko Hayashi and Matthias Eschrig for valuable discussions. T. Dahm acknowledges funding from a research grant for young scientists of the University of Tübingen.

- 
- [1] L. Kramer and W. Pesch, Z. Physik **269**, 59-64 (1974).
  - [2] N. Hayashi, Y. Kato and M. Sigrist, J. Low Temp. Phys. **139**, 79 (2005)
  - [3] J. Kortus, I. I. Mazin, K. D. Belashchenko, V. P. Antropov and L. L. Boyer, Phys. Rev. Lett. **86**, 4656 (2001).
  - [4] A. Y. Liu, I. I. Mazin and J. Kortus, Phys. Rev. Lett. **87**, 087005 (2001).
  - [5] E. J. Choi, D. Roundy, H. Sun, M. L. Cohen and S. G. Louie, Nature (London) **418**, 758 (2002).
  - [6] For a recent review see T. Dahm in *Frontiers in Superconducting Materials*, ed. A. V. Narlikar, pp. 983-1009, Springer 2005 (cond-mat/0410158).
  - [7] N. Schopohl and K. Maki, Phys. Rev. B **52**, 490 (1995).
  - [8] N. Schopohl, in *Quasiclassical Methods in the Theory of Superconductivity and Superfluidity*, Bayreuth, Germany, 1998, edited by D. Rainer and J. A. Sauls, cond-mat/9804064 (unpublished).
  - [9] F. Gygi and M. Schlüter, Phys. Rev. B **43**, 7609 (1991).
  - [10] M. Ichioka, M. Takigawa and K. Machida in *Vortices in Unconventional Superconductors and Superfluids*, eds. R. P. Hübener, N. Schopohl and G. E. Volovik, pp. 225-242, Springer 2002.
  - [11] M. Abramowitz and I. A. Stegun, *Handbook of Mathematical Functions*, chapter 6, Dover (New York 1972).
  - [12] K. Usadel, Phys. Rev. Lett. **25**, 507 (1970).
  - [13] A. E. Koshelev and A. A. Golubov, Phys. Rev. Lett. **90**, 177002 (2003).
  - [14] M. Eschrig, J. Kopu, A. Konstantin, J. C. Cuevas, M. Fogelström, and G. Schön, *Advances in Solid State Physics* Vol. **44**, pp. 533-546, Springer Verlag, Heidelberg (2004).
  - [15] M. G. Vavilov and A. I. Larkin, Phys. Rev. B **67**, 115335 (2003).
  - [16] For a review see C. T. Rieck, K. Scharnberg, and

- N. Schopohl, J. Low Temp. Phys. **84**, 381 (1991).
- [17] T. Dahm and N. Schopohl, Phys. Rev. Lett. **91**, 017001 (2003).
  - [18] S. V. Shulga, S.-L. Drechsler, H. Eschrig, H. Rosner and W. E. Pickett, cond-mat/0103154.
  - [19] S. Graser, T. Dahm, and N. Schopohl, Phys. Rev. B **69**, 014511 (2004).
  - [20] C. Iniotakis, private communication.
  - [21] I. I. Mazin, O. K. Andersen, O. Jepsen, O. V. Dolgov, J. Kortus, A. A. Golubov, A. B. Kuz'menko, and D. van der Marel, Phys. Rev. Lett. **89**, 107002 (2002).
  - [22] J. W. Quilty, S. Lee, S. Tajima, and A. Yamanaka, Phys. Rev. Lett. **90**, 207006 (2003).
  - [23] I. Pallecchi, V. Braccini, E. G. d'Agliano, M. Monni, A. S. Siri, P. Manfrinetti, A. Palenzona, and M. Putti, Phys. Rev. B **71**, 104519 (2005).
  - [24] M. Eschrig, contributed talk at the Spring Meeting of the German Physical Society, Berlin (2005).